

AD-A146 537

THE EFFECT OF POTENTIAL ON THE CORROSION FATIGUE
BEHAVIOR OF A PRECIPITAT.. (U) RENSSELAER POLYTECHNIC
INST TROY NY DEPT OF MATERIALS ENGINEE..

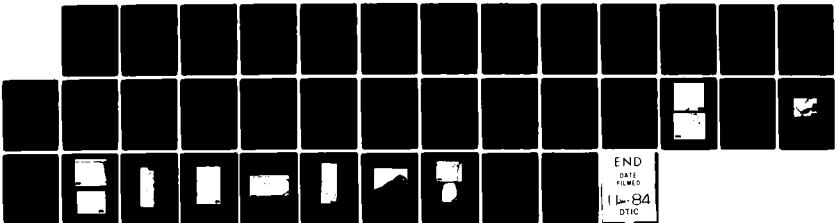
1/1

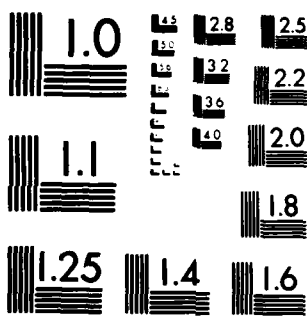
UNCLASSIFIED

E F SMITH ET AL. SEP 84 15

F/G 20/11

NL





MICROCOPY RESOLUTION TEST CHART
NATIONAL BUREAU OF STANDARDS-1963-A

AD-A146 537

(12)

TECHNICAL REPORT TO THE OFFICE OF NAVAL RESEARCH

CONTRACT N00014-67-A-0117-0012
No. N00014-75-C-0466, NR 036-093

THE EFFECT OF POTENTIAL ON THE CORROSION FATIGUE
BEHAVIOR OF A PRECIPITATION HARDENED ALUMINUM ALLOY

BY

E.F. Smith, III and D.J. Duquette
Rensselaer Polytechnic Institute
Materials Engineering Department
Troy, New York 12180-3590

September 1984

REPRODUCTION IN WHOLE OR IN PART FOR ANY PURPOSE OF THE U.S. GOVERNMENT
IS PERMITTED. DISTRIBUTION OF THIS DOCUMENT IS UNLIMITED.

DTIC FILE COPY

SEARCHED
SERIALIZED
OCT 9 1984
A

84 10 03 025

REPORT DOCUMENTATION PAGE		READ INSTRUCTIONS BEFORE COMPLETING FORM
1. REPORT NUMBER 15	2. GOVT ACCESSION NO. AD-A1465	3. RECIPIENT'S CATALOG NUMBER 37
4. TITLE (and Subtitle) The Effect of Potential on the Corrosion Fatigue Behavior of a Precipitation Hardened Aluminum Alloy.	5. TYPE OF REPORT & PERIOD COVERED ANNUAL	
7. AUTHOR(s) E.F. Smith, III and D.J. Duquette	6. PERFORMING ORG. REPORT NUMBER	
9. PERFORMING ORGANIZATION NAME AND ADDRESS Rensselaer Polytechnic Institute Troy, New York 12181	8. CONTRACT OR GRANT NUMBER(s) N00014-67-A-0117-0012	
11. CONTROLLING OFFICE NAME AND ADDRESS Office of Naval Research Arlington, VA 22217	10. PROGRAM ELEMENT, PROJECT, TASK AREA & WORK UNIT NUMBERS	
14. MONITORING AGENCY NAME & ADDRESS (if different from Controlling Office)	12. REPORT DATE September 1984	
	13. NUMBER OF PAGES 33	
16. DISTRIBUTION STATEMENT (of this Report) Reproduction in whole or in part for any purpose of the U.S. Government is permitted. Distribution of this document is unlimited.	15. SECURITY CLASS. (of this report) Unclassified	
	15a. DECLASSIFICATION/DOWNGRADING SCHEDULE	
17. DISTRIBUTION STATEMENT (of the abstract entered in Block 20, if different from Report)		
18. SUPPLEMENTARY NOTES		
19. KEY WORDS (Continue on reverse side if necessary and identify by block number) Corrosion Fatigue Al Alloys		
20. ABSTRACT (Continue on reverse side if necessary and identify by block number) → Fatigue experiments were conducted on polycrystalline and monocrystalline samples of a high purity Al-5.5 w/o Zn, 2.5 w/o Mg, 1.5 a/o Cu alloy in the peak-hardened heat treatment condition. These experiments were conducted in dry laboratory air and in 0.5 N NaCl solutions at the corrosion potential and at applied potentials cathodic (continued on back)		

→ to the corrosion potential. It has been shown that saline solutions severely reduce the fatigue resistance of the alloy, resulting in considerable amounts of intergranular crack initiation and propagation under freely corroding conditions for polycrystalline samples. Applied cathodic potentials resulted in still larger decreases in fatigue resistance and, for polycrystals, increased the degree of transgranular crack initiation of propagation. ← Increasing amounts of transgranular cracking were also observed when applied cyclic stresses were reduced (longer test times). The characteristics of cracking, combined with results obtained on tensile tests of deformed and hydrogen charged samples suggest that environmental cracking of these alloys is associated with a form of hydrogen embrittlement of the process zone of cracks. Further, it is suggested that stress corrosion cracking and corrosion fatigue of these alloys occurs by essentially the same mechanism but that the often observed transgranular cracking under cyclic loading conditions occurs due to enhanced hydrogen transport and/or solubility associated with mobile dislocations at growing crack tips.

ABSTRACT

Fatigue experiments were conducted on polycrystalline and monocrystalline samples of a high purity Al - 5.5 w/o Zn, 2.5 w/o Mg, 1.5 a/o Cu alloy in the peak-hardened heat treatment condition. These experiments were conducted in dry laboratory air and in 0.5 N NaCl solutions at the corrosion potential and at applied potentials cathodic to the corrosion potential. It has been shown that saline solutions severely reduce the fatigue resistance of the alloy, resulting in considerable amounts of intergranular crack initiation and propagation under freely corroding conditions for polycrystalline samples. Applied cathodic potentials resulted in still larger decreases in fatigue resistance and, for polycrystals, increased the degree of transgranular crack initiation of propagation. Increasing amounts of transgranular cracking were also observed when applied cyclic stresses were reduced (longer test times). The characteristics of cracking, combined with results obtained on tensile tests of deformed and hydrogen charged samples suggest that environmental cracking of these alloys is associated with a form of hydrogen embrittlement of the process zone of cracks. Further, it is suggested that stress corrosion cracking and corrosion fatigue of these alloys occurs by essentially the same mechanism but that the often observed transgranular cracking under cyclic loading conditions occurs due to enhanced hydrogen transport and/or solubility associated with mobile dislocations at growing crack tips.

Introduction

It has been well established that high strength precipitation hardened aluminum alloys are highly sensitive to environmental degradation of their mechanical properties. This degradation can be exhibited as ductility loss, as spontaneous crack propagation under static loading (SCC) or as an increase in crack propagation rates under dynamic loading (CF). It has been noted that these alloys are sensitive to humid gaseous as well as liquid phase aqueous environments, and that, under a number of circumstances pre-exposure of the alloys to these environments may also lead to ductility losses.⁽¹⁻⁶⁾ In general, the presence of chloride ion in the environment renders the alloys still more sensitive to environmental degradation as do increases in the aggressivity of the environment. To date, however, there have been few studies which have successfully linked each of these phenomena, although it has been suggested that hydrogen, generated by interaction of the alloy with its environment, may be responsible for the observed degradation. This point has been disputed, however, and Ford has pointed out that, when corrosion studies of simulated crack tips are performed by either anodic or cathodic polarization, the actual reaction rate limiting process on the alloy surface is, at best, ambiguous.⁽⁷⁻⁹⁾ A further complication arises in that most observed ductility losses which have been observed experimentally still show significant amounts of dimpled rupture on transgranular surfaces (indicating a significant amount of conventional ductility), while SCC generally exhibits intergranular failure. Corrosion fatigue generally

occurs in a transgranular mode with what appears to be extensive stage I or crystallographic cracking. However, even in this case, the situation is complicated, since it has been observed that the corrosion fatigue fracture path shifts from the normally observed (111) fatigue fracture plane to either a (100) or (112) plane.(10,11) Even in only mildly aggressive environments such as moist air a shift in fracture path has been shown for single crystals, the latter observation being highly sensitive to test frequency (and presumably time of exposure relative to time available for crack advance).(12,14)

The present study examines the effects of cathodic potentials and subsequent hydrogen evolution on the fatigue characteristics of polycrystalline and monocrystalline high purity Al-Zn-Mg-Cu alloys.

Experimental Procedure

Load controlled fatigue tests were performed on a high purity Al-Zn-Mg-Cu alloy in 0.5N NaCl solution as functions of electrochemical potential. The composition of the alloy was aluminum with 5.5 w/o Zn, 2.5 w/o Mg and 1.5 w/o Cu. Cast material was hot rolled to 2.5mm and subsequently cold rolled to 1.9mm. Specimens of gauge length 12.7mm and width of 5mm were cut from the rolled sheet. After machining the specimens were solution heat treated for three hours at 738°K, cold water quenched and aged for 24 hours at 393°K. Specimen surfaces were mechanically and electrochemically polished prior to testing.

For a few tests single crystal of the alloy were prepared by using a strain anneal technique. Sheets of 38mm x 51mm x

89mm were heat treated at 743°K for 3 hours, cold water quenched and strained to 2-4%. After straining the sheets were re-solution heat treated at 743°K. This technique yielded grain diameters of the order of 6-7mm, sufficient to have a single grain in the specimen gauge section.

Tensile test results of the polycrystalline samples indicated that the alloy was within the specification for a commercial 7075-T6 alloy ($\sigma_y = 500$ MPa, $\sigma_{UTS} = 570$ MPa). Tensile tests of the single crystals indicated that the majority of the crystals produced by strain anneal were oriented for single slip and in fact, Laue analyses of all of the large crystals produced indicated that all but one of the crystals had orientations which were near the center of the conventional stereographic projection triangle. The critical resolved shear stress of the alloy crystals was measured as 144 ± 15 MPa.

Fatigue tests were performed in a tension-tension mode (R~0) at 30 Hz with a constant mean stress of 207 MPa. Tests were conducted in dry laboratory air or in aerated 3% NaCl solutions, as a function of applied electrochemical potential. Potentials were referred to a saturated calomel electrode (SCE) and currents were measured from a Pt mesh counter electrode attached to the inner diameter of a cylindrical 0.5l plexiglas cell. Solutions were recirculated from a 20l reservoir at the rate of approximately 0.5l/min.

Optical and electron microscopic examinations were conducted on external specimen surfaces and on fracture surfaces.

Results

a. Polycrystals

The results of exposure to a 3% NaCl solution during cyclic loading are shown in Figure 1. Specific data points are deleted for clarity. Comparative fracture surfaces for the alloy are shown in Figure 2. Fatigue crack initiation in air is characterized by crystallographic cracking followed by river line formation of feathery river lines emanating from the crack initiation region. In many cases cracks initiate in these equiaxed grain specimens in grain boundaries, but no cases of more than a single grain boundary separation were observed. A grain boundary initiation site is shown as A in Figure 2a. specimens tested in 3% NaCl solution, at the corrosion potential, in contrast to tests conducted in dry air, often show significant amounts of grain boundary separation near the initiation site (Figure 2b). Another distinguishing feature of the fracture surface developed in the NaCl solution is the character of the river lines. In the aqueous chloride solution the river lines are generally more distinct, and the extent of a single set of river lines is confined to a single grain. This implies that the crystallography of river line formation is more defined under conditions of corrosion fatigue. Additionally, striations formed under corrosive conditions are of the brittle type described by other investigators. (10,11)

Cathodic polarization of the alloy in the saline solutions to -1.3 volts vs. SCE, the limiting potential of the $H^+ + e^- \rightarrow \frac{1}{2} H_2$ reaction, and the beginning of the reduction of H_2O to

form H_2 and OH^- resulted in no significant change in the fatigue behavior from that observed under freely corroding conditions. However, at more active potentials (-1.5 volts and -1.75 volts vs. SCE), a significant reduction in fatigue resistance is observed, with a greater reduction in fatigue resistance being observed at more active potentials (Figure 3). In addition to the observed reductions in fatigue lives, the fractographic features of the alloy are considerably different under conditions of cathodic polarization. For example, at the corrosion potential, for a moderately large applied cyclic stress, the fracture initiation process, and early crack propagation occur by intergranular separation while, at the most cathodic potential, cracking is entirely transgranular. These results are shown in Table I. It should be noted, however, that this transition from intergranular crack initiation and early propagation is also a function of the applied cyclic stress level. For example, Table II shows that, at -1.75 volts vs. SCE, decreasing the cyclic stress range (while maintaining the mean stress at a constant level) results in increasing amounts of intergranular cracking. Figure 4 shows a transition region for a specimen held at -1.75 volts vs. SCE and shows that cracking occurs in a mixed mode with significant amounts of transgranular cracking. However, it should be noted that the secondary intergranular cracking which is observed does not appear to be due to enhanced corrosion since the details of the fracture surface are so sharply defined.

B. Single Crystals

The results of corrosion fatigue studies of single crystals

of the aluminum alloy under conditions of either free corrosion or of cathodic charging closely paralleled the results obtained for polycrystals. Figure 5 shows a plot of the resolved shear stress for each single crystal vs. the number of cycles to failure. The tensile axis orientation was determined by post test analyses of specimens failed by corrosion fatigue processes. Figure 5 was developed by normalizing the corrosion fatigue data of polycrystalline specimens under free corrosion conditions with the single point obtained for a single crystal under free corrosion conditions. This procedure established the positioning of the data obtained in dry air and at a cathodic potential of -1.75 volts vs. SCE. It can be seen from these data that the general trends are maintained surprisingly well given the indefinite orientation of the single crystals governed by the strain anneal method of production. *Fractographs of two of the single crystals tested at applied electrochemical potentials of -1.3 and -1.75 volts vs. SCE respectively are shown in Figure 6 and the principal differences in surface morphology are that, apparently, at the more active potential, cyclic cleavage is more extensive and more clearly defined.*

Only a single specimen was tested in the multiple slip orientation, [approximately (110)]. This specimen showed somewhat different fracture surface topographic features than those tested in the single slip orientation. In this case, fracture progresses along a primary crystallographic fracture plane, deviates from this plane in a classic river line pattern, and returns to the primary fracture plane. Thus, a "banded" structure is formed.

The "bands", which define the single fracture plane, become narrower as the crack propagates. Figure 7a and b show the topography of this orientation change, and Figure 8 shows a cross sectional view of the fracture surface. The serendipitous etch pitting process of the primary fracture plane, which occurs preferentially on the featureless crystallographic bands clearly identifies this fracture plane as having the (100) orientation (Figure 9).

Discussion

The results of this investigation have shown that the corrosion fatigue phenomenon in high strength aluminum alloys is accelerated by cathodic potentials. Further, the results have shown that, while exposure to aqueous chloride solutions significantly reduces fatigue resistance, polarization of the alloy to a potential greater than 500mv active to the corrosion potential, results in no further degradation of fatigue resistance. In fact, in another study on a commercial alloy, it has been shown there is a small but significant amount of cathodic protection in the potential range between the corrosion potential and the -1300mv (vs. SCE) potential value.⁽¹⁾ This previous study also provided strong support for the concept that hydrogen embrittlement was the primary cause of corrosion fatigue failure in these alloys, since pre-exposure to corrosive solutions followed by baking yielded considerable reversibility of the corrosion fatigue process. It is significant to note that at potentials noble to -1300mv vs. SCE, the primary source of hydrogen is the hydronium ion in solution, additionally, evolution of hydrogen

in this potential range occurs at such a slow rate that no significant pH changes occur on the alloy surface. However, at more active potentials significant amounts of OH^- are liberated through the reduction of water according to the conventional reaction $\text{H}_2\text{O} + \text{e}^- \rightarrow \frac{1}{2} \text{H}_2 + \text{OH}^-$. This increase in local pH attacks the otherwise protective aluminum oxide film and allows hydrogen to enter the lattice and/or grain boundaries. It should be noted that this instability of the protective film also increases the corrosion rate of the alloy, however, it is not believed that this increase in corrosion rate, per se is responsible for the reduction in fatigue resistance. For example, a simple increase in corrosion rate of the alloy surface should not result in the observed differences in fracture morphology as functions of potential or cyclic stress range. Also, an increased corrosion rate caused by pH changes cannot explain the shift in crack initiation and early propagation path to intergranular or, if it is assumed that increased general corrosion rates alter the relative corrosion behavior of grain boundaries vs. grains, cannot explain the transition from IG to TG propagation with increasing crack length. Similarly the cyclic stress related transition from TG to IG initiation with lower cyclic stresses cannot be explained by a model which simply involves increased corrosion rates. Rather, it is suggested that hydrogen may enter the alloy more readily if the protective film is dissolved. Enhanced diffusion in grain boundary vs. lattice diffusion is a well known phenomenon. More active potentials release more hydrogen. However, because of the low cross sectional area of the grain

boundary, this easy diffusion path should be rapidly saturated with hydrogen at very active potentials. This saturation would tend to increase the relative amount of hydrogen in the lattice and, if hydrogen is in fact responsible for local embrittlement, the crack path should accordingly shift to a transgranular mode, as is observed.

The effect of cyclic stress can be explained in a similar manner if it is assumed that either dislocation or slip band enhanced diffusion can occur. As in the aforementioned case, this action would be considered to alter the relative distribution of hydrogen in the alloy. At low applied cyclic stresses the preferred diffusion path would tend to be grain boundaries and grain boundary initiation would be expected. As the cyclic stress is increased, the to-and-fro motion of dislocations in active slip bands would tend to increase the concentration of hydrogen in the bands. For these alloys this action would be particularly damaging since it has been shown by several authors that slip is confined to very narrow deformation bands.(15-18) This action also explains the transition from IG to TG cracking, for low nominal applied cyclic stresses. As the crack lengthens the increasing K would tend to behave in the same manner as a high applied nominal stress on the surface of the alloy.

The single crystal results support a model of this type. For example, in the absence of grain boundaries, cracking is by necessity transgranular and follows a crystallographic path; in particular the (100) plane. This is especially evident in the crystal which was not oriented for single slip. In this

case, a zone of material appears to be essentially "sensitized" ahead of the crack tip. As the crack grows in the zone, the crack propagation rate increases until it reaches such a rate that the "sensitized" zone is overrun. At this point, the crack propagation rate decreases allowing time for the "sensitized" zone to develop. During this period the crack advances along the principal (111) slip band. Thus, a banded structure is produced. It is significant to note that, in contrast with many other crack morphologies, the bands become narrower with increasing crack propagation rates. It is believed that the environmentally affected crack path occurs preferentially along the (100) plane since intersecting (111) slip planes would effectively "pump" hydrogen to this plane and cause separation.

Additionally, it should be noted that the phase boundary between $MgZn_2$ and the aluminum matrix has been shown to be primarily associated with the (100) or (110) plane of the matrix.⁽¹⁹⁾ It is accordingly suggested that hydrogen is effectively delivered to these interfaces, collects and results in interfacial separation. This suggestion is supported by the observations of Montgrain and Swann which showed that, in moist air, interphase separation occurs along the incoherent interfaces between $MgZn_2$ and a grain boundary (in the absence of significant amounts of plastic deformation).⁽²⁰⁾

The results of this and the referenced complementary investigation appear to rule out the possibility that corrosion is fundamentally responsible for corrosion fatigue crack growth in alloys of this type.⁽¹⁾ In this related study, Jacko has

shown that the corrosion fatigue process is partially reversible. Also, Gerold and co-workers have shown similar changes in crack surface orientations in single crystals as functions of frequency and moisture content of the environment.(12-15) In aqueous solutions de-stabilization of the passive film either allows sufficient hydrogen to be generated to embrittle the alloy or more likely, allows ready ingress of hydrogen into the alloy. In the absence of cathodic potentials where significant amounts of caustic solution are generated which reduce the passive film and generate copious amounts of hydrogen, chloride ion alone damages the passive film and results in localized corrosion where hydrogen is evolved and allows hydrogen ingress.

This work also appears to provide a link between SCC and corrosion fatigue (CF) of these high strength Al alloys. A particular complication of this comparison has traditionally been that SCC is invariably IG while CF is generally observed to be TG. Also in CF the fracture plane is observed to occur along non-slip planes such as (112) or (100).(10,11) The model proposed herein suggests that at low cyclic stresses, or where the hydrogen fugacity is low, the grain boundary provides a preferential hydrogen diffusion and collection path and TG separation occurs. For higher cyclic stresses and high fugacities (such as is provided by cathodic charging) dislocation transport and/or lattice diffusion increase the bulk hydrogen concentration, allows for hydrogen collection at precipitate interfaces, and transgranular separation occurs. The action of either chloride ion or of caustic generation by cathodic charging is either to

locally or generally damage the protective film, and to increase the hydrogen concentration in the near surface of the alloy (for crack initiation) or in the vicinity of growing crack tips (for crack propagation).

As a further test of this hypothesis several related experiments were performed on polycrystal and single crystal samples in uniaxial tensile loading. These experiments were conducted in aqueous solutions of $1N$ H_2SO_4 + $0.2 N$ AsO_3 at an applied cathodic potential of -1.75 volts vs. SCE. It was noted that, in order to embrittle the alloy, an applied tensile stress in excess of the yield stress was necessary. If the alloy was simply charged with hydrogen and subsequently tensile tested, no effect was observed. However, if the alloy was hydrogen charged, strained to yield and held at a constant load, subsequent loading resulted in serrated yielding and in intergranular separation with very limited plasticity. In fact, in the T-6 condition failure occurred at a stress level which was below the previously determined yield stress (after stress relaxation) (Figure 10a). Small amounts of ductility were only observed in the T-0 condition (Figure 10b). For the single crystal test, both serrated yielding and low ductility were observed (Figure 10c) and, surprisingly, IG failure occurred in a grain boundary approximately 0.5 cm from the cathodically charged crystal (under a lacquer mask). This result strongly supports a hydrogen transport process to the grain boundary by plastic deformation. It should be noted that, although the fractures observed were identical to those generally reported for SCC, the alloy was

not exposed to chloride ion at any time during the experiment.

Additionally, for the single crystal in the T-0 condition, serrated yielding was observed in subsequently loading following the yield, plus constant stress experiment (Figure 10b). This indicates a solute-dislocation interaction and provides further evidence that (a) hydrogen is dissolved in the lattice and (b) hydrogen may be transported by plastic deformation. Finally, even single crystals tested in this manner showed extensive reductions in plasticity when compared with tests performed in laboratory air.

Conclusions

The results of this study provide strong evidence that hydrogen is associated with stress corrosion cracking and corrosion fatigue of precipitation hardened aluminum alloys. For example, it has been shown that:

1. The degree of corrosion fatigue damage is highly dependent on the amount of hydrogen available at the alloy surface (liberated by cathodic charging).
2. The fracture morphology is dependent on both available hydrogen and cyclic stress levels, less general hydrogen availability and low applied stress levels resulting in significant intergranular failure. These results indicate that hydrogen transport may be rate limiting.
3. Solid solution dissolved hydrogen interacts with mobile dislocations resulting in serrated yielding. However, hydrogen is not dissolved in the alloy unless the protective passive film is either chemically (with halide) or mechanically breached.

4. Corrosion fatigue and stress corrosion cracking of these high strength aluminum alloys is cationically sensitive only insofar as chloride ion attacks the passive film and either directly liberates hydrogen as the cathodic reaction in a corrosion couple or allows hydrogen ingress by exposing the alloy surface.
5. The specific high sensitivity of Al-Mg-Zn alloys in contrast to Al-Zn, Al-Mg or Al-Cu precipitation hardened alloys appears to be due to the specific crystallography and internal stress fields of the $MgZn_2$ precipitates.

Acknowledgements

The authors would like to acknowledge the support of the U.S. Office of Naval Research under Contract No. 100015-75-C-0466 and in particular the encouragement of Dr. P.A. Clarkin.

Table I

Effect of Applied Cathodic Potential in the
Fracture Morphology of Al-5.5Zn-2.5Mg-1.5Cu
Alloy in 0.5 N NaCl Solution

<u>Potential (V vs. SCE)</u>	<u>% Intergranular Failure</u>
-.780 (corrosion potential)	23
-1.300	5
-1.750	0

Table II

Effect of Cyclic Load (at Constant Mean Stress)
on the Fracture Morphology of Al-5.5Zn-2.5Mg-1.5Cu
Alloy in 0.5M NaCl Solution at a Cathodic Potential
of -1.75V vs. SCE

<u>Cyclic Stress MPa</u>	<u>% Intergranular Failure</u>
76	0
69	0
55	0
41	10
28	26
17	35

References

1. R.J. Jacko, Ph.D. Dissertation, Rensselaer Polytechnic Institute, Troy, New York (1975).
2. J. Albrect, A.W. Thompson and I.M. Bernstein, *Met. Trans.*, 10A, 1759, (1979).
3. D. Hardie, N.J.H. Holroyd and R.N. Parkins, *Met. Sci.*, 13, 603 (1979).
4. N.J.H. Holroyd and D. Hardie, *Corrosion Sci.*, 21, 129 (1981).
5. S.W. Ciaraldi, Ph.D. Dissertation, University of Illinois, Champaign-Urbana, Illinois (1980).
6. R. Gest, Ph.D. Dissertation, Case-Western Reserve University, Cleveland, Ohio (1972).
7. F.P. Ford, *Corrosion*, 35, 281 (1979).
8. F.P. Ford, *Met. Sci.*, 12, 326 (1978).
9. F.P. Ford, G.T. Burstein and T.P. Hoar, *J. Electrochem. Soc.*, 127, 1325 (1980).
10. C.A. Stubbington and P.J.E. Forsyth, *J. Inst. of Metals*, 90, 347 (1961).
11. C.A. Stubbington, *Metallurgia*, 65, 109 (1963).
12. M. Nageswararao and V. Gerold, *Met. Trans.*, 7A, 1847 (1977).
13. M. Nageswararao and V. Gerold, *Met. Sci.*, 11, 31 (1977).
14. M. Nageswararao, R. Meyer, M. Wilhelm and V. Gerold in "Mechanisms of Environment Sensitive Cracking of Materials", Surrey, p.383 (1977).
15. W. Vogel, M. Wilhelm and V. Gerold, *Acta Met.*, 30, 31 (1982).
16. D.J. Duquette and P.R. Swann, *Acta Met.*, 24, 241 (1976).
17. W. Vogel, M. Wilhelm and V. Gerold, *Acta Met.*, 30, 21 (1982).
18. P.J.E. Forsyth, *Acta Met.*, 11, 703 (1963).
19. J. Gjønnes and C.J. Simensen, *Acta Met.*, 18, 881 (1970).
20. L. Montgrain and P.R. Swann in "Hydrogen in Metals", Ed. J. Bernstein and A. Thompson, *Am. Soc. for Metals*, Ohio (1974) p.575.

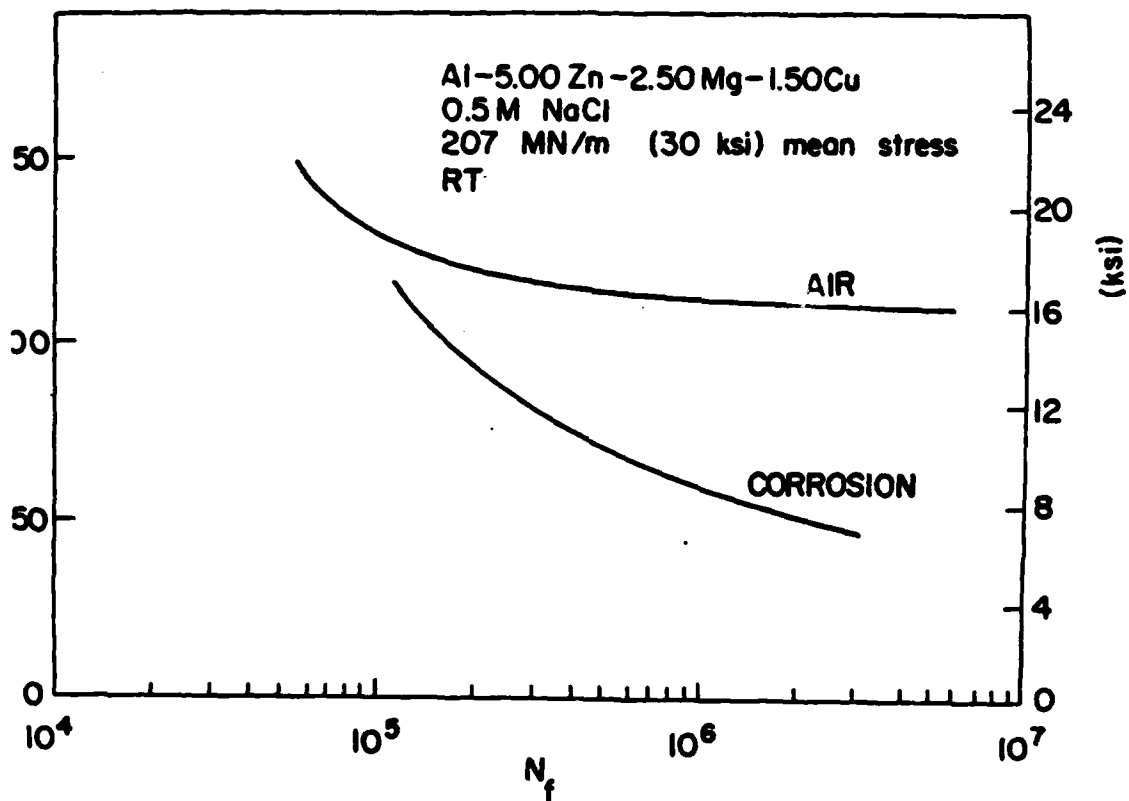


Figure 1. S-N behavior of a polycrystalline Al-5Zn-2.5Mg-1.5Cu alloy heat treated to the T-6 condition in dry air and in 0.5 M NaCl. The specific data points are not shown in order to clarify the trends.

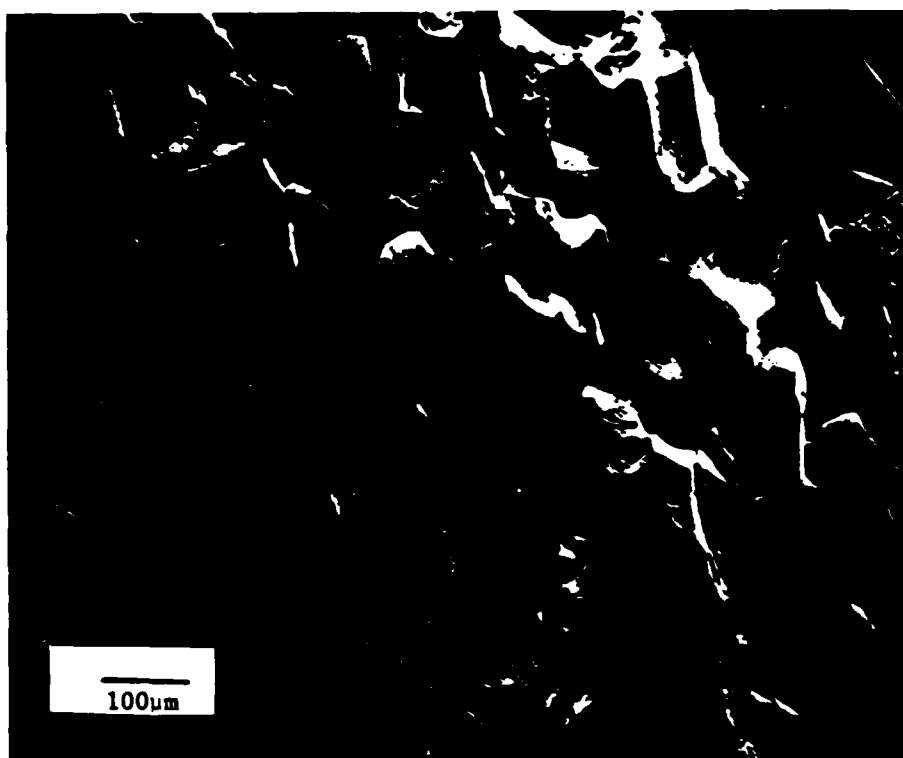
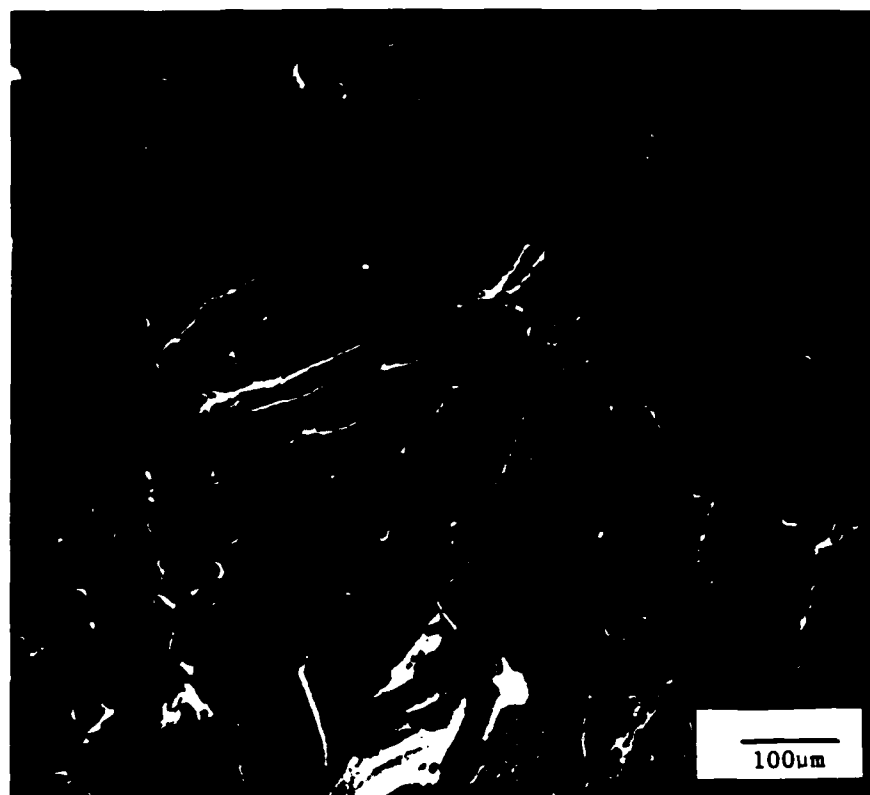


Figure 2. Typical fracture surfaces of Al-5Zn-2.5Mg-1.5Cu alloy fatigued to failure (a) in air and (b) in 0.5 M NaCl solution at the corrosion potential.

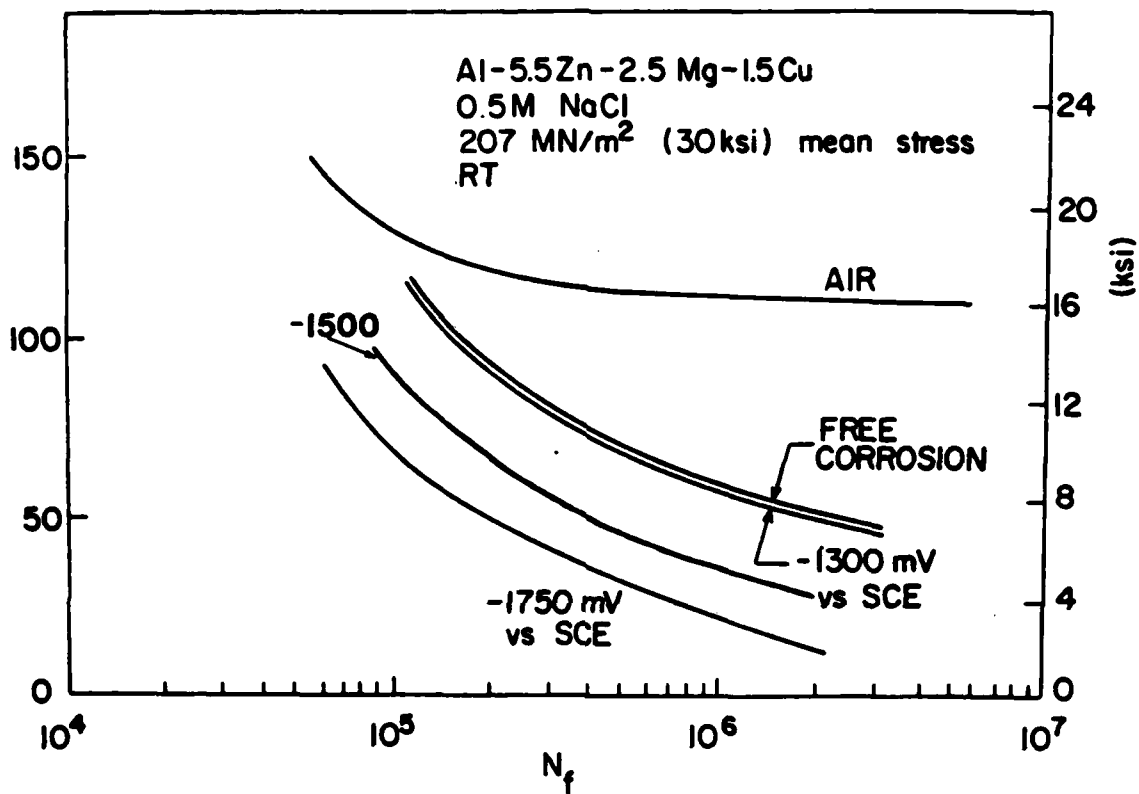


Figure 3. S-N Behavior of polycrystalline Al-5Zn-2.5Mg-1.5Cu alloy tested in 0.5 M NaCl as a function of applied cathodic potentials.

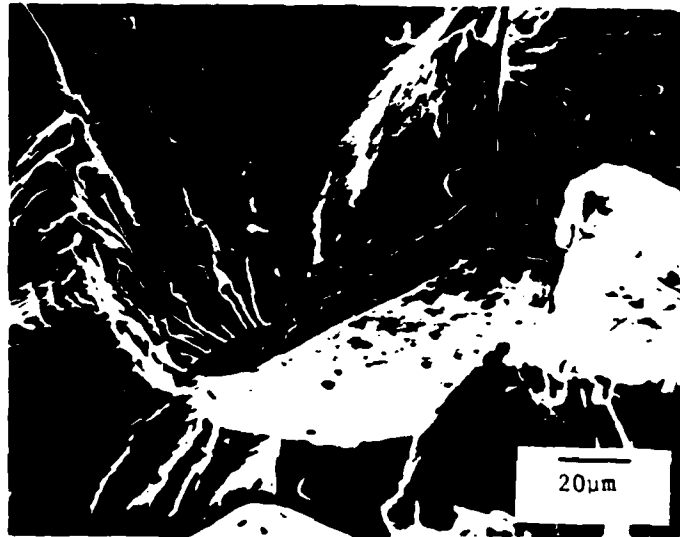


Figure 4. Fracture surface of Al-5Zn-2.5Mg-1.5Cu Alloy at $-1.75V$ vs. SCE showing mixed cracking mode and secondary cracking near the fatigue-overload region. The arrow denotes the direction of fatigue crack growth.

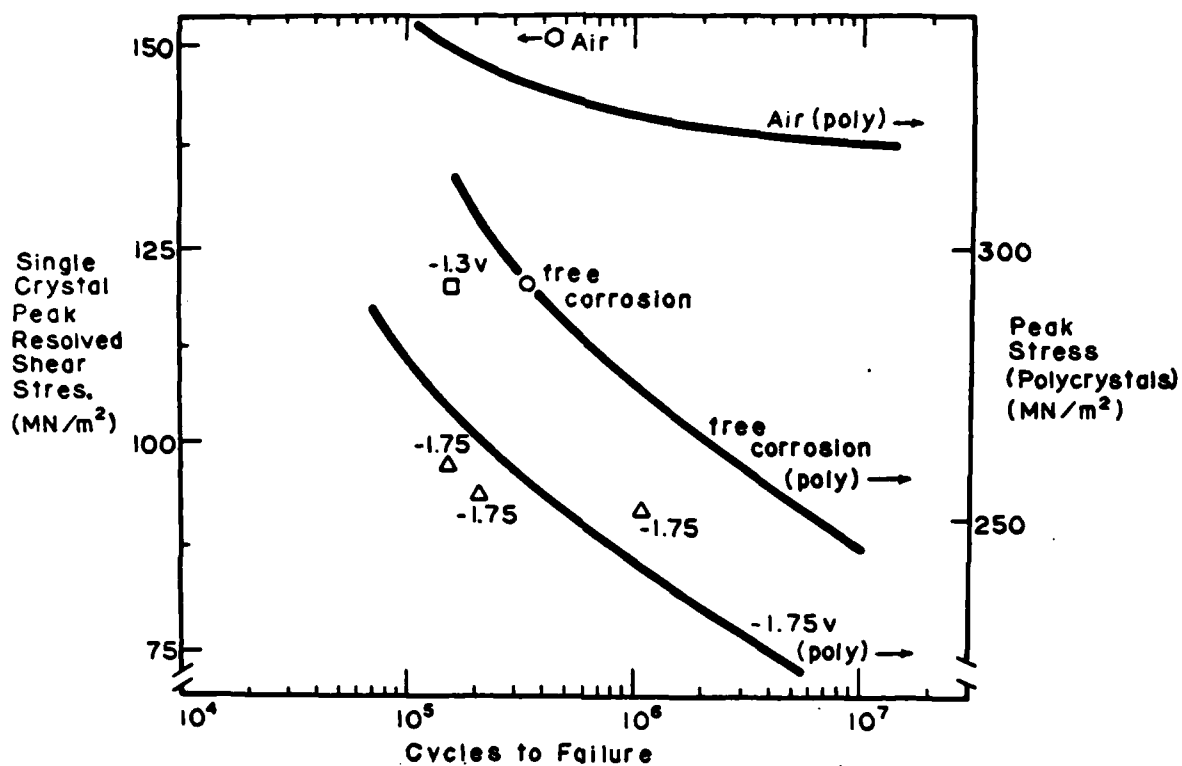
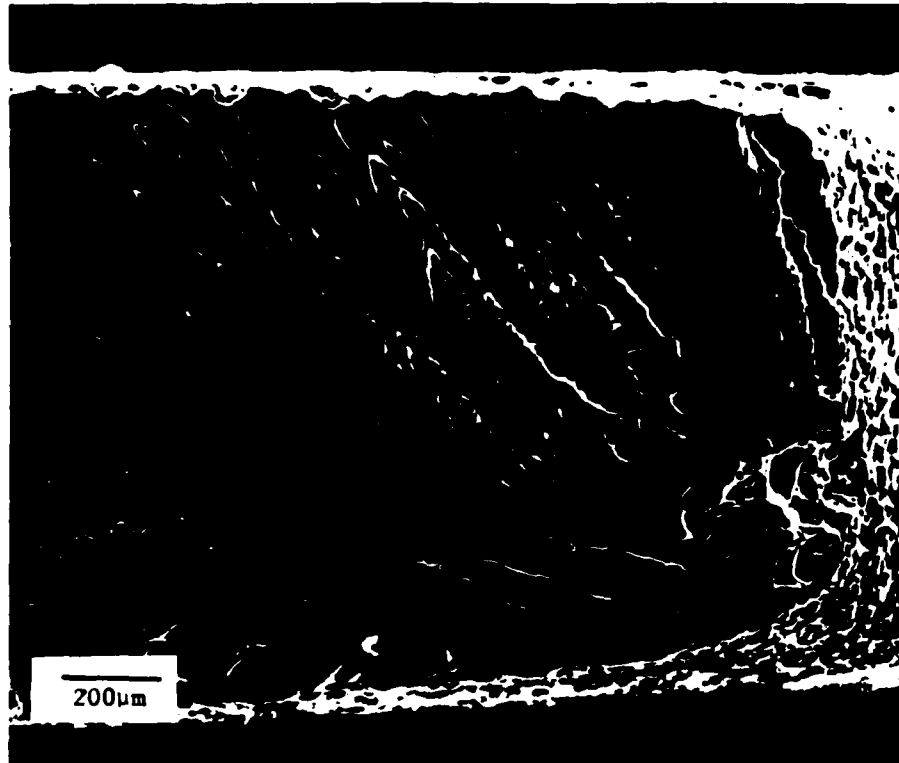
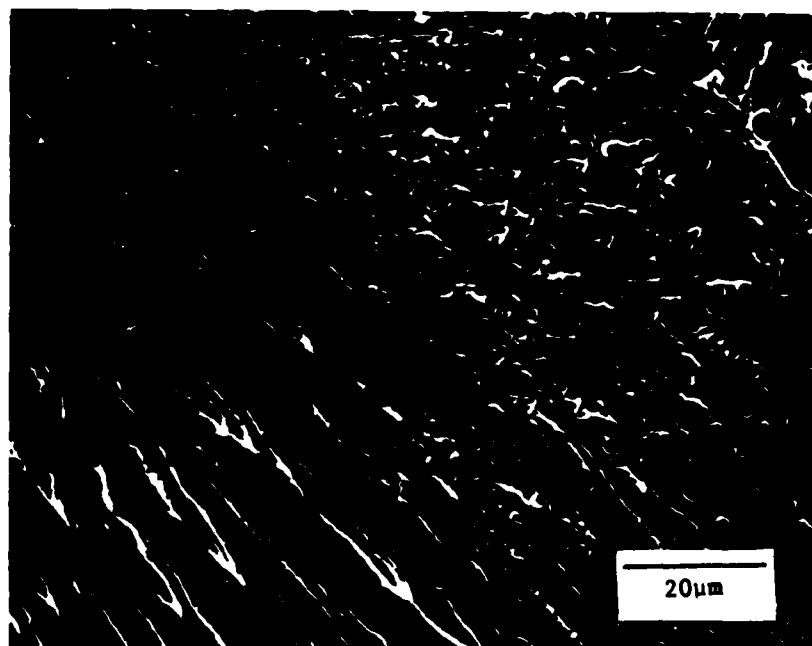


Figure 5. Resolved shear stress versus cycles to failure for single crystals of Al-5.5Zn-2.5Mg-1Cu in 0.5 M NaCl solution as a function of potential. The data are normalized by superimposing the polycrystalline data on the single crystal data at the free corrosion potential.



(a)
200μ=1.4



(b)
20μ=2cm

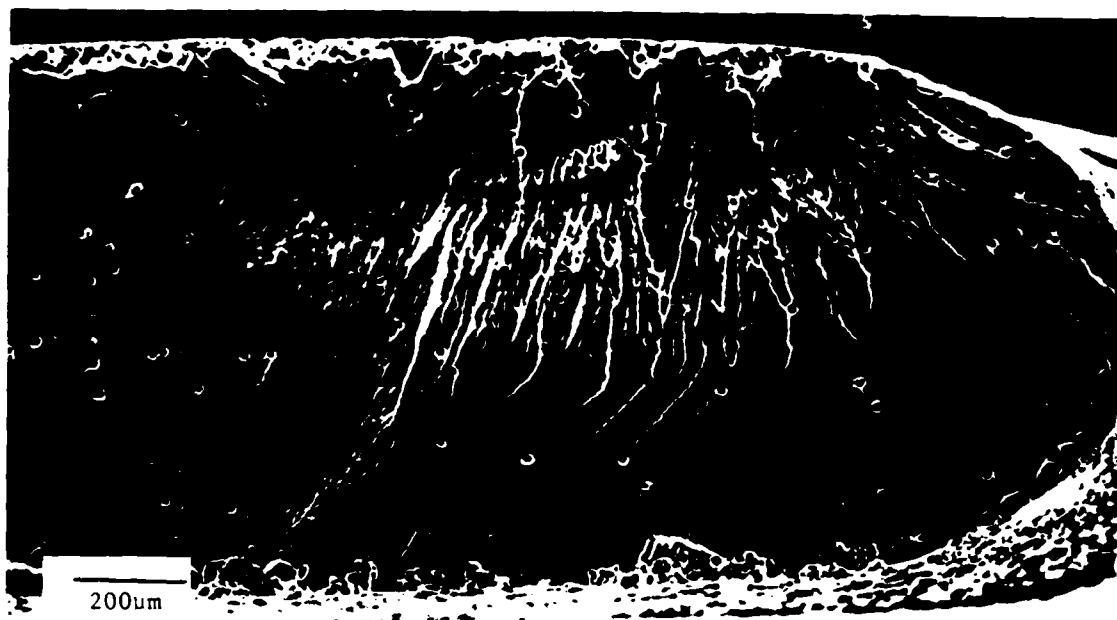
Figure 6. Fractographs of cathodically polarized single crystals of Al-5.5Zn-2.5Mg-1.5Cu alloy (a and b) -1.3 vs. SCE and (c and d) -1.75 vs. SCE. The arrows in (a) and (c) indicate fatigue crack initiation sites, while the black lines in (b) show the direction of crack growth.



(6c)



(6d)



(7a)

Figure 7(a&b) Fractographs of a cathodically polarized (-1.75V) single crystal of Al-5.5Mg-2.5Zn-1.5Cu alloy, in the (110) tensile axis orientation showing an alternating fracture path and multiple initiation sites (a).



(7b)



Figure 8. (a) Cross-sectional view of fracture surface shown in Figure 7. The black lines indicate the (111) fracture planes between the environmentally affected cleavage-like surfaces.

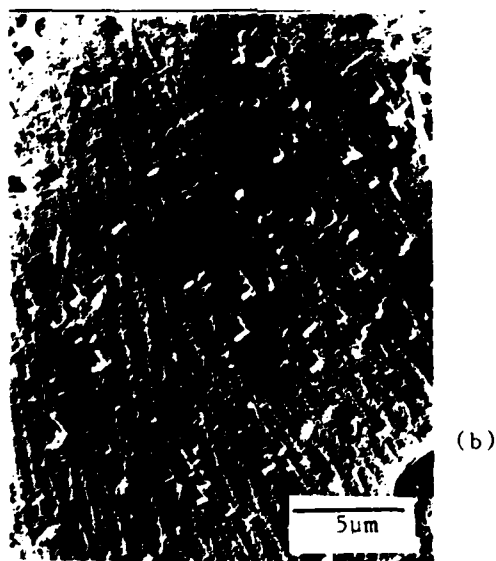
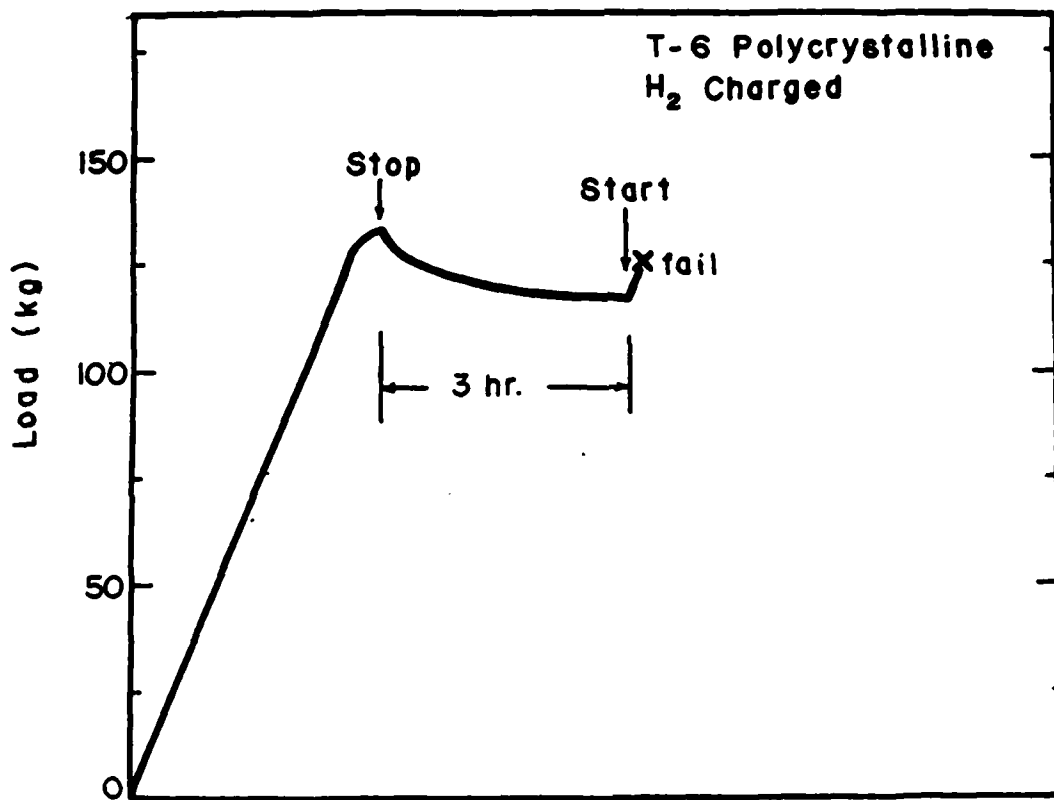
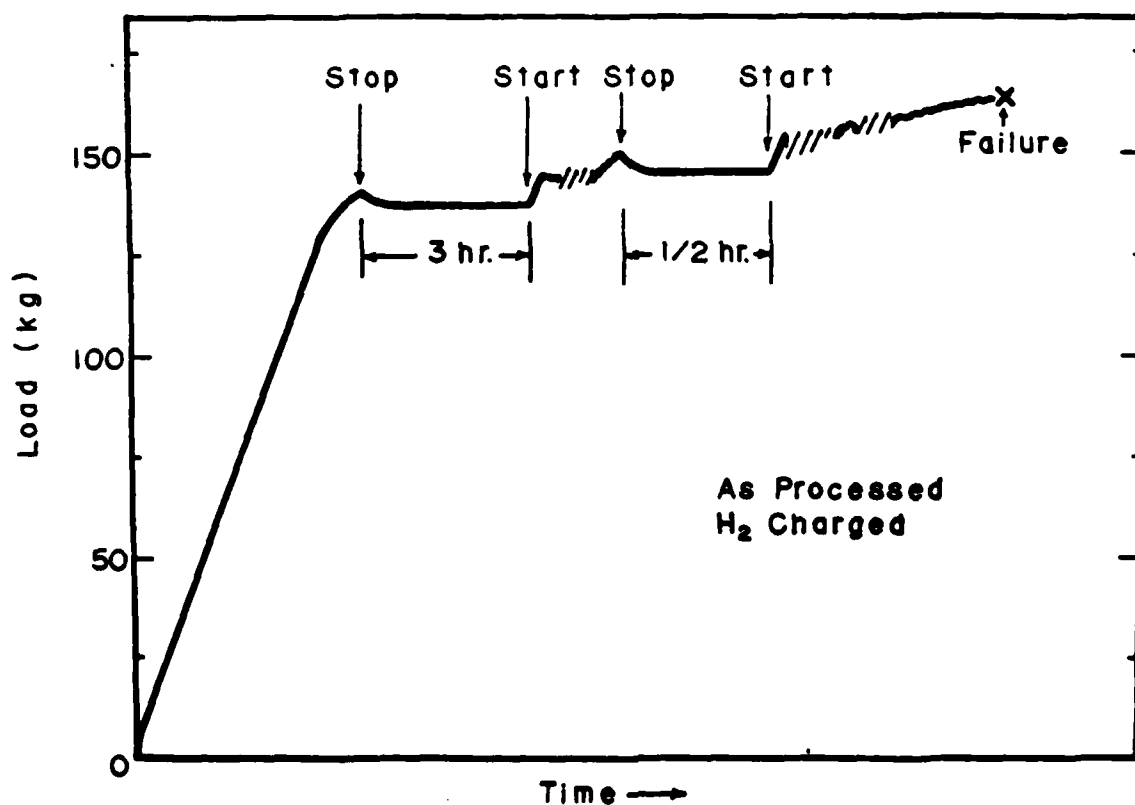


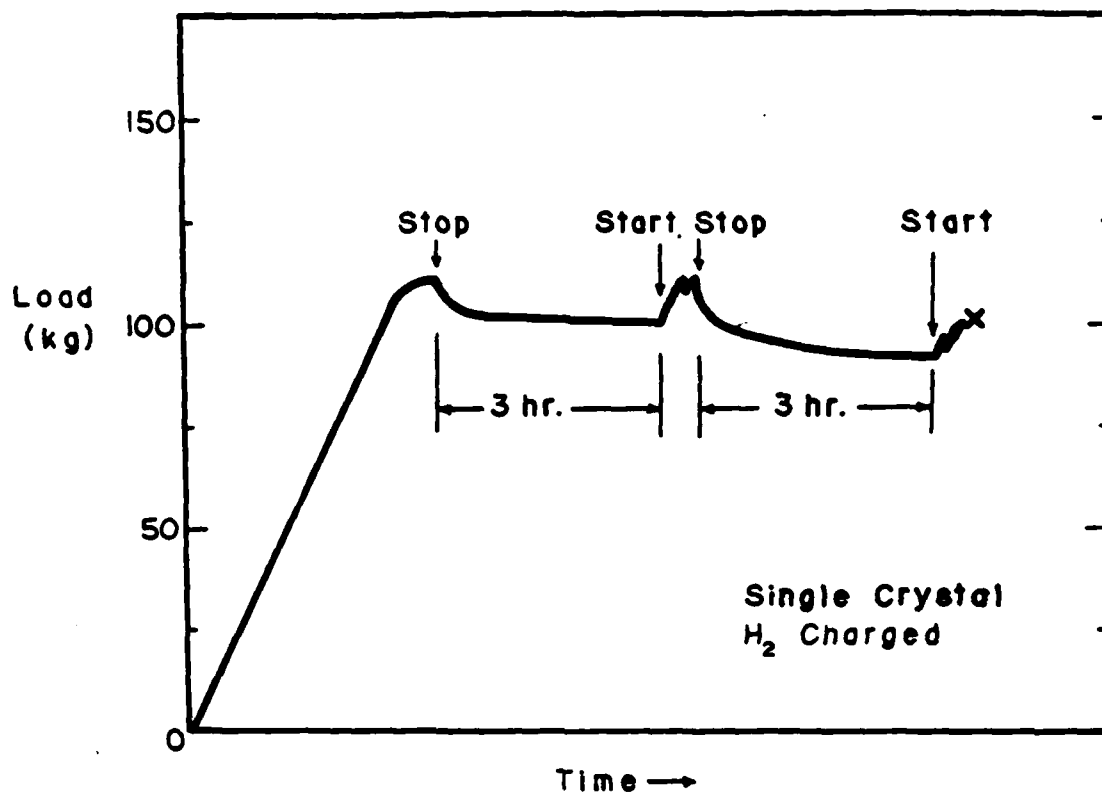
Figure 9. Detailed fractograph of figure 7 showing cubically oriented etch pits on the fracture surface. (a) SEM (b) carbon replica.



(10a)



(10b)



(10c)

Figure 10. Loading, load relaxation and reloading diagram for a polycrystalline alloy in the T-6 aged condition, tested in 1 N H_2SO_4 + 0.2 N $NaAsO_3$ at -175V vs. SCE (b) As in (a) except for an alloy in the T-0 (as processed) heat treatment (c) As in a except for a single crystal aged to the T-6 heat treatment.

4